Bioorganic & Medicinal Chemistry 19 (2011) 5490–5499

Contents lists available at ScienceDirect

Bioorganic & Medicinal Chemistry

journal homepage: www.elsevier.com/locate/bmc

2-({6-[(3*R*)-3-amino-3-methylpiperidine-1-yl]-1,3-dimethyl-2,4-dioxo-1,2,3,4-tetrahydro-5*H*-pyrrolo[3,2-*d*]pyrimidine-5-yl}methyl)-4-fluorobenzonitrile (DSR-12727): A potent, orally active dipeptidyl peptidase IV inhibitor without mechanism-based inactivation of CYP3A

Yukihiro Nishio *, Hidenori Kimura, Naoyuki Sawada, Eiji Sugaru, Masakuni Horiguchi, Michiko Ono, Yudai Furuta, Mutsuko Sakai, Yumi Masui, Misato Otani, Takahiko Hashizuka, Yayoi Honda, Jiro Deguchi, Tsutomu Nakagawa, Hiroyuki Nakahira

Drug Research Division, Dainippon Sumitomo Pharma Co. Ltd, 3-1-98 Kasugade Naka, Konohana-ku, Osaka 554-0022, Japan

ARTICLE INFO

Article history:
Received 6 June 2011
Revised 22 July 2011
Accepted 22 July 2011
Available online 4 August 2011

Keywords:
DPP IV inhibitors
Mechanism-based inactivation

ABSTRACT

We report on the identification of 2-({6-[(3*R*)-3-amino-3-methylpiperidine-1-yl]-1,3-dimethyl-2,4-dioxo-1,2,3,4-tetrahydro-5*H*-pyrrolo[3,2-*d*]pyrimidine-5-yl}methyl)-4-fluorobenzonitrile (DSR-12727) (**7a**) as a potent and orally active DPP-4 inhibitor without mechanism-based inactivation of CYP3A. Compound **7a** showed good DPP-4 inhibitory activity (IC_{50} = 1.1 nM), excellent selectivity against related peptidases and other off-targets, good pharmacokinetic and pharmacodynamic profile, great in vivo efficacy in Zucker-fatty rat, and no safety concerns both in vitro and in vivo.

1. Introduction

Type 2 diabetes (T2D) is a major metabolic disorder affecting approximately 194 million people worldwide. This number is estimated to reach 366 million by 2030.[1] The beneficial effects of antidiabetic agents currently used, such as sulphonylurea, biguanide, and α-glucosidase inhibitors that can effectively increase insulin secretion or decrease glucose absorption are known to be associated with a number of side effects including hypoglycemia, weight gain, gastrointestinal disorders, and lactic acidosis. Thus, current treatments for T2D are considered to be unsatisfactory in terms of prevention of complications and preservation of quality of life.[2] Under these circumstances, intensive effort has been made to find better and safer drugs for T2D.

Glucagon-like peptide 1 (GLP-1), an important incretin hormone that regulates body blood glucose, has recently been receiving great attention as a new target for the development of novel therapies for T2D.[3] However, the active state of GLP-1 (7–36) is short-lived as this hormone is quickly cleaved by dipeptidyl peptidase IV (DPP-4).[4] This means that DPP-4 inhibition, and consequently increase in GLP-1 level, presents a new approach for the treatment of T2D. DPP-4, a serine protease distributed throughout the body, modulates the activity of a wide variety of regulatory peptides. Based on the report about DPP-4 knockout mice, the use of DPP-4 inhibition in T2D therapy seems to have lots of advantages.[5–7] It is suggested that DPP-4 inhibitors might be able to stimulate production of new β-cell in patients with T2D, and thus prevent deterioration of the disease. In addition, DPP-4 inhibition is unlikely to cause serious hypoglycemia, because GLP-1 is strictly glucose-dependent.

In recent years, a number of DPP-4 inhibitors,[8] such as **1** (sitagliptin),[9] **2** (vildagliptin),[10] **3** (saxagliptin),[11] **4** (alogliptin),[12] and **5** (linagliptin),[13] (Fig. 1) have been marketed or are under clinical development, and have shown great efficacy in patients with T2D.

In our research about DPP-4 inhibitors, we found compound **6**,[14] which showed excellent inhibitory activity against DPP-4 (0.34 nM), however, had two pharmacokinetic drawbacks. One is reversible inhibition of Cytochrome P450 (CYP) 3A4 (IC_{50} = 1.6 μM), CYP1A2 (IC_{50} = 14.7 μM), and CYP2D6 (IC_{50} = 7.5 μM) caused by the parent drug. The other is potent mechanism-based inactivation (MBI)[15] which is irreversible inhibition of CYP3A. MBI is time- and concentration-dependent CYP enzymes inhibition, and caused by metabolites of original compounds. Some specific structures, such as nitroso species, to coordinate with the Fe-center of CYP enzymes or bind covalently with it have been reported as the cause of MBI, however, few examples to prevent or alleviate potent MBI have been reported.[16] Our investigation about metabolites of compounds having

* Corresponding author. Tel.: +81 6 6466 5223; fax: +81 6 6466 5287.
E-mail address: yukihiro-nishio@ds-pharma.co.jp (Y. Nishio).

0968-0896/$ - see front matter © 2011 Elsevier Ltd. All rights reserved.
doi:10.1016/j.bmc.2011.07.042

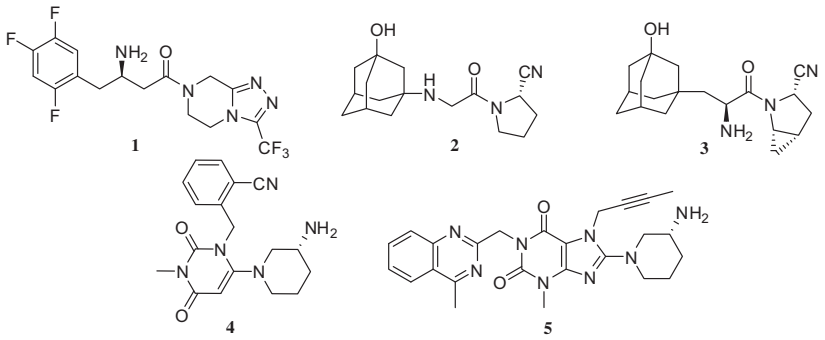

Figure 1. Structures of known DPP-4 inhibitors.

the (*R*)-3-aminopiperidine unit, which includes **6**, revealed that metabolism of these compounds mainly undergo at the uracil structure to give demethylated compounds, at the piperidine moiety to give hydroxylated derivatives and at the (*R*)-3-amino position of the piperidine unit to give hydroxyl amine. Among them, hydroxyl amine is supposed to give nitroso species, which is believed to form a metabolic intermediate complex and cause MBI.[16,17]

We have previously reported new chemotype DPP-4 inhibitors having (*R*)-3-amino-3-methylpiperidine as a pharmacophore and showed that these inhibitors have good in vitro activity and pharmacokinetic/pharmacodynamic (PK/PD) profiles.[18] In addition to those results, a methyl substitution seemed to have good influence on CYP enzymes inhibition because the reported compounds hardly had strong inhibition of CYP enzymes. Thus, it was expected that compound **6** strong inhibition of CYP3A4 would be alleviated by it. As for MBI, we assumed that introduction of a small alkyl substituent at the 3-position of piperidine unit could prevent metabolism at the amino group and/or coordinate of reactive metabolites with the Fe-center of CYP3A to avoid MBI. We therefore considered that compound **7a**, having a methyl instead of a hydrogen at 3-position of compound **6** piperidine unit, would become an ideal DPP-4 inhibitor. In addition, to compare the effects of a small alkyl substituent on the inhibitory activity and potent MBI, the ethyl substituted compound **7b** was also prepared and evaluated (Fig. 2). Here, we disclosed our evaluation of these compounds, and the identification of 2-({6-[(3*R*)-3-amino-3-methylpiperidine-1-yl]-1,3-dimethyl-2,4-dioxo-1,2,3,4-tetrahydro-5*H*-pyrrolo[3,2-*d*]pyrimidine-5-yl}methyl)-4-fluorobenzonitrile (DSR-12727) (**7a**) as a potent and orally active DPP-4 inhibitor without mechanism-based inactivation of Cytochrome P450 3A.

2. Results and discussion

2.1. Chemistry

The 3-amino-3-alkyl-piperidine structures **13a–b** were synthesized in four steps.[18] The intermediate **9b** was prepared from ethyl nipecotate **8** same as **9a**.[19] The nitrogen-atom of **9a–b** was protected by a carbobenzyloxy (Cbz) to give **10a–b**, which were hydrolyzed to afford the carboxylic acid **11a–b**. After Curtius rearrangement using diphenylphosphoric azide (DPPA), the crude solution was first washed with water to remove by-products, and then treated with an excess amount of *tert*-butyl alcohol and a catalytic amount of potassium *tert*-butoxide to give **12a–b**. The Cbz group at the 1-amino position was removed by hydrogenation to afford the target amines (*R*)-3-amino-3-methylpiperidine (**13a**) and *rac*-3-amino-3-ethylpiperidine moiety (**13b**) (Scheme 1).

Compounds **6**, **7a**, and **7b** were prepared in five steps. The intermediate **15a–c** was prepared from starting material **14** as previously described.[20] The pyrrole moiety of **15a–c** was treated with KOCN to give an urea intermediate, which was first cyclized and then methylated under basic condition to provide **16a–c**. Cyanation of **16a–c** gave **17a–c**, and the final structures **6**, **7a** and *rac*-**7b** were obtained by removal of the *tert*-butoxy carbonyl (Boc) group and the *tert*-butyl ester at the C7-position using benzensulphonic acid. Each enantiomer of **7b**, (+)-**7b**, and (−)-**7b**, were prepared by chiral separation at Daicel Chemical Industries, Ltd (http://www.daicel.co.jp/) (Scheme 2). Absolute configurations of following enantiomers, **7a**, (+)-**7b**, and (−)-**7b**, have not been determined, and configurations written in this article are supposed by the synthetic ways, inhibitory activities, and the information of other DPP-4 inhibitors, such as **4**[12] and **5**.[13]

2.2. Influence on in vitro potency

The in vitro DPP-4 inhibitory activity of the compounds listed in Table 1 was measured using human plasma DPP-4. To evaluate our compounds DPP-4 inhibitory activity, some approved drugs (**1**, **2**, and **4**) were used as reference. The parent compound **6** showed a strong DPP-4 inhibitory activity (IC_{50} = 0.34 nM), being almost two-fold that of **2** (IC_{50} = 0.58 nM). As for compound **7a** having (*R*)-3-amino-3-methyl piperidine, its DPP-4 inhibitory activity (IC_{50} = 1.1 nM) was three-fold less than that of **6**, but almost the same as that of **4** (IC_{50} = 1.0 nM). The ethyl substituted compound (+)-**7b** on the other hand showed a DPP-4 inhibitory activity (IC_{50} = 26 nM) 80-fold less than that of the parent compound **6**. The other enantiomer (−)-**7b** did not have any inhibition against DPP-4. Based on these findings, only the methyl substituted compound **7a** could retain an acceptable DPP-4 inhibitory activity as we expected. To maintain strong in vitro DPP-4 inhibitory, the sub-

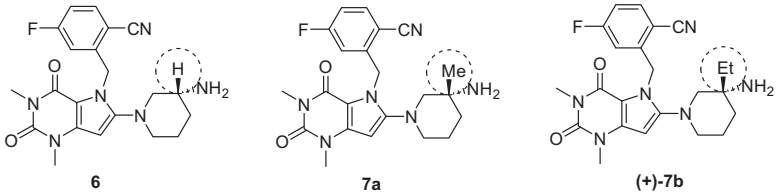

Figure 2. Structures of test-compounds.

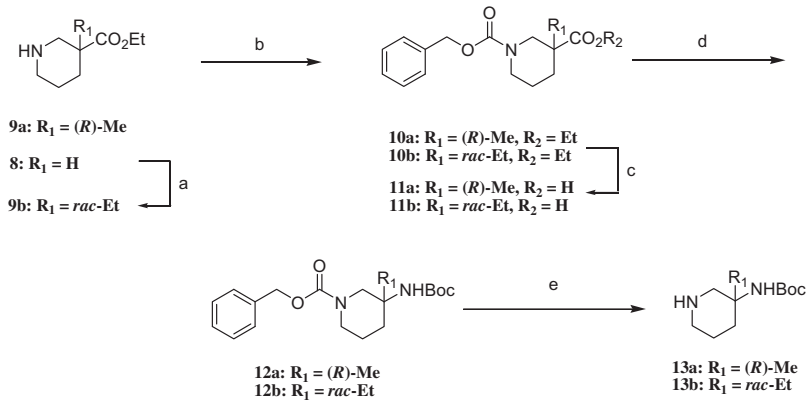

Scheme 1. Synthetic route for tetra-substituted amines. Reagents and conditions: (a) NaHMDS (1.2 equiv), EtI (1.0 equiv), toluene, −20 °C – rt; (b) CbzCl (1.0 equiv), Et_3N (1.5 equiv), THF, rt, overnight; (c) 3 N NaOH aq, THF, MeOH, reflux, 1 day for **10a**, 3 days for **10b**; (d) DPPA (1.0 equiv), Et_3N, toluene, 100 °C, 1 h, then *t*-BuOK (0.1 equiv), *t*-BuOH, 40 °C, 3 h; (e) Pd/C, H_2, MeOH, rt, 3 h.

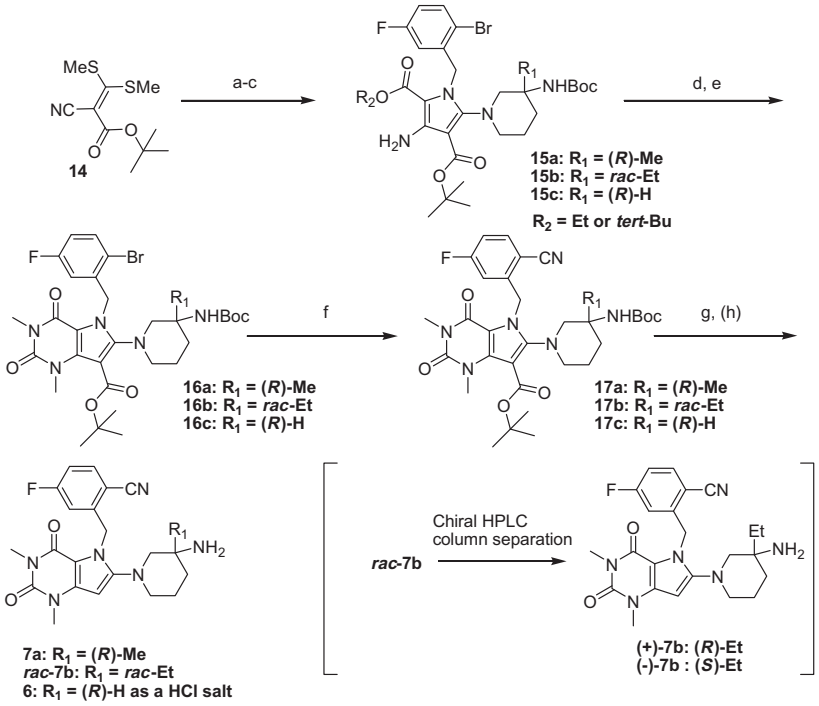

Scheme 2. Synthetic route for the pyrrolo[3,2-*d*]pyrimidine structure. Reagents and conditions: (a) **13a**, **13b** or *tert*-butyl [(*R*)-3-piperidine-3-yl]carbamate (1.0 equiv, respectively), CH_3CN, 50 °C, 1 h, then 2-bromo-5-fluorobenzyl amine (1.2 equiv), DBU (2.0 equiv), CH_3CN, 80 °C, 10 h; (b) ethyl bromoacetate (1.3 equiv), K_2CO_3 (3.0 equiv), DMF, 50 °C, 2 h; (c) $LiNH_2$ (2.5 equiv), *t*-BuOH (20 equiv), CH_3CN, 30 °C, 2 h; (d) KOCN (1.6 equiv), AcOH, 40 °C, 2 h; (e) K_2CO_3 (1.6 equiv), DMF, 50 °C, 5 h, then MeI (2.0 equiv), K_2CO_3 (1.6 equiv), 30 °C, 2 h; (f) Pd(*t*-$Bu_3P)_2$ (0.1 equiv), $Zn(CN)_2$ (0.6 equiv), NMP, 100 °C, 1 h; (g) $PhSO_3H$ monohydrate (2.0 equiv), CH_3CN, 80 °C, 2 h; (h) only for **6**, 1.0 N HCl aq, MeOH, H_2O, rt.

Table 1
In vitro inhibitory activity of DPP-4 inhibitors

Compound	IC_{50} (nM)
1	3.5
2	0.58
4	1.0
6	0.34
7a[a]	1.1
(+)-**7b**[a]	26
(−)-**7b**[a]	>1.000

[a] Absolute configuration has not been determined.

stituent at the 3-position of the piperidine had to be kept small. As it has been shown that the (*R*)-3-aminopiperidine of **4**[12] and **5**[13] interact with Glu205, Glu206, and Tyr662 of the enzyme, we assumed that an ethyl substituent might influence this interaction, or the conformation of piperidine, more than a methyl substituent.

2.3. Estimation of the potency of mechanism-based inactivation (MBI)

MBI for CYP enzymes is considered as a risk of drug–drug-interaction (DDI). However, in clinical usage not all compounds showing MBI are subject to DDI.[21] In general, compounds potential for DDI can be evaluated using MBI kinetic parameters.[22] The apparent constant inactivation ratio (k_{obs}) is estimated from the initial slope of a plot of the natural log of the remaining enzymatic activity

Table 2
Test-compounds MBI kinetic parameters

Compound	k_{inact} (min^{-1})	K_I (nμ)	k_{inact}/K_I (min^{-1}/nM)
b	0.0391	0.026	1.50
7a	N.A.[a]	N.A.[a]	–
(+)-**7b**	0.0227	0.022	1.03

[a] N.A. means not applicable. No clear change was observed

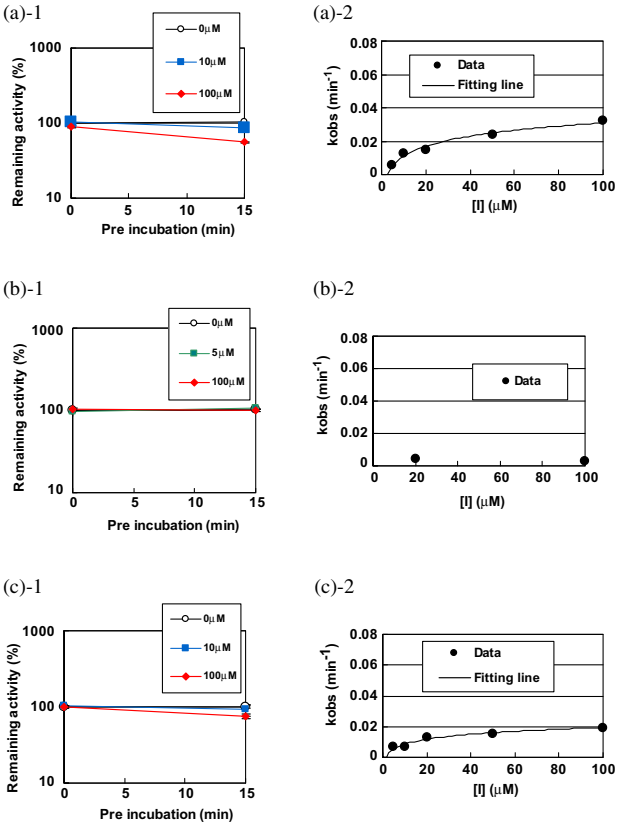

Figure 3. MBI parameter of each test-compound; (a) **6**, (b) **7a**, and (c) (**+**)-**7b**. [1] CYP3A remaining activity plotted against pre-incubation-time and [2] relationship between kobs and inactivator concentration [*I*].

against pre-incubation time. The maximum inactivation rate constant (k_{inact}) and the inactivator concentration at half-maximal rate of enzyme inactivation (K_I) are determined by the non-linear least squares fitting of Eq. (1). [*I*] is the inactivator concentration.

$$k_{obs} = (k_{inact}[I])/(K_I + [I]) \quad (1)$$

In our research, k_{inact}/K_I ratio has been used to compare a given compound MBI potency.[22] Before measuring our compounds k_{inact}/K_I ratio, other DPP-4 inhibitors were assayed to investigate effects of pharmacophore differences on MBI. While compounds **1**, **2**, and **3** does not show any MBI potency, **4** and **5** having (*R*)-3-amino piperidine same as **6**, have potent MBI (k_{inact}/K_I = 4.1 for **4** and 8.8 for **5**, respectively). These results strongly support our assumption that (*R*)-3-aminopiperidine is the cause of MBI.

MBI kinetic parameters of compounds **6**, **7a**, and (+)-**7b** for CYP3A are given in Table 2. Compound **6** has k_{inact}/K_I ratio less than those of **4** and **5**. As expected, compound **7a** with a methyl substituent showed no change in MBI kinetic parameters, but, contrary to our expectations, compound (+)-**7b** exhibited an MBI approximately 70% lower than that of **6**. This decrease in MBI was more associated with decreased k_{inact} value than K_I value (Fig. 3).

Table 3
Pharmacokinetic profile of **7a** in the rat, dog, and monkey

Species	dose (mg/kg)	CL (mL/min/kg)	C_{max} (ng/mL)	V_{dss} (L/kg)	$t_{1/2}$ (h)	B.A. (%)
Rat	1[a]	40	–	6.5	4.1	–
	3[b]	–	76	–	3.3	52
Dog	1[a]	29	–	5.8	3.1	–
	3[b]	–	245	–	3.9	91
Monkey	1[a]	38	–	10	4.8	–
	3[b]	–	77	–	15	38

[a] Test compounds were administered intravenously.
[b] Test compounds were administered orally.

At first, we assumed that steric hindrance created by the alkyl substituent prevented metabolism of the amino group. However, this hypothesis could not accord with the case of an ethyl group. This led us to investigate the metabolites of **7a**. Like in compound **6**, we found that metabolism of **7a** occurred at the 3-amino position and gave a hydroxyl amine as one of the metabolites. When a dansyl Glutathione (dGSH) trapping assay to detect reactive metabolites of **7a** was carried out, production of 0.14 μM dGSH adduct was observed. These findings indicate that the methyl substituent does not prevent metabolism, but only affects coordination with the Fe-center of CYP3A to give MI complex. The reason why compound (+)-**7b** having ethyl substituent did not prevent MBI completely same as compound **7a** is unclear and under investigation now. However, the drop in k_{inact} of (+)-**7b** was observed, and the result means that introduction of steric hindrance at the metabolism sites supposed to give reactive metabolites might reduce or avoid the risk of MBI. Based on these results, for example, DPP-4 inhibitory activity and potent MBI, compound **7a** was selected for further evaluation.

2.4. Compound 7a selectivity against DPP-4 related peptidases and off-targets

Before investigating the pharmacokinetics (PK) of compound **7a**, the selectivity of this compound against DPP-4 related peptidases and potential off-targets, for example muscarinic receptor 1,[13] 2, and 4[23] was evaluated. Compound **7a** showed great selectivity against DPP-4 related peptidases, such as dipeptidyl peptidase II (DPP-2)[24], dipeptidyl peptidase VIII (DPP-8),[25] dipeptidyl peptidase IX (DPP-9),[26,27] prolidase, prolyl oligpeptidase (POP), fibroblast activation protein alpha (FAPα),[28] and aminopeptidase P (Amino. P) (IC_{50} >50 μM). As for compound **7a** selectivity against off-targets, a thorough evaluation using Pharma Screen® showed no affinity for a wide variety of receptors, including muscarinic receptor 1, 2, and 4 (IC_{50} >10 μM).

As compound **6** had concerns about inhibition against CYP enzymes and hERG[18], these profiles of compound **7a** were evaluated. Compound **7** showed weak inhibition of hERG (IC_{50} = 30 μM) and had no or only weak in vitro CYP enzymes inhibition (CYP 1A2, 2A6, 2C8, 2C9, 2C19, and 3A4; IC_{50} >50 μM, CYP 2D6; IC_{50} = 38 μM). These result let us to carry out further studies of compound **7a**.

2.5. Pharmacological evaluation of 7a

PK profile of compound **7a** was assessed in the rat, dog, and monkey (Table 3). Compound **7a** showed great bioavailability (B.A.) in dogs (91%) and moderate B.A. in rats and monkeys (52% and 38%, respectively). Compound **7a** systemic clearance (CL) and maximal concentration (C_{max}) in rats (40 mL/min/kg and 76 ng/mL, respectively) were similar to those in monkeys (38 mL/min/

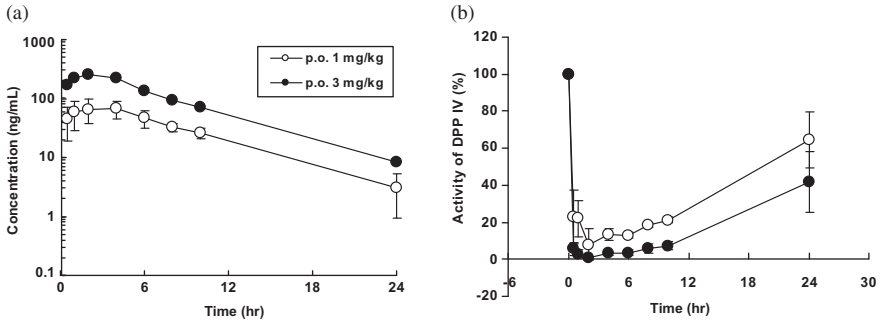

Figure 4. PK/PD profile of **7a** in ZF rats; (a) time course of plasma concentration and (b) plasma DPP-4 activity after oral administration of compound **7** in rats. Each vertical bar represents the means ±SD (n = 4–5).

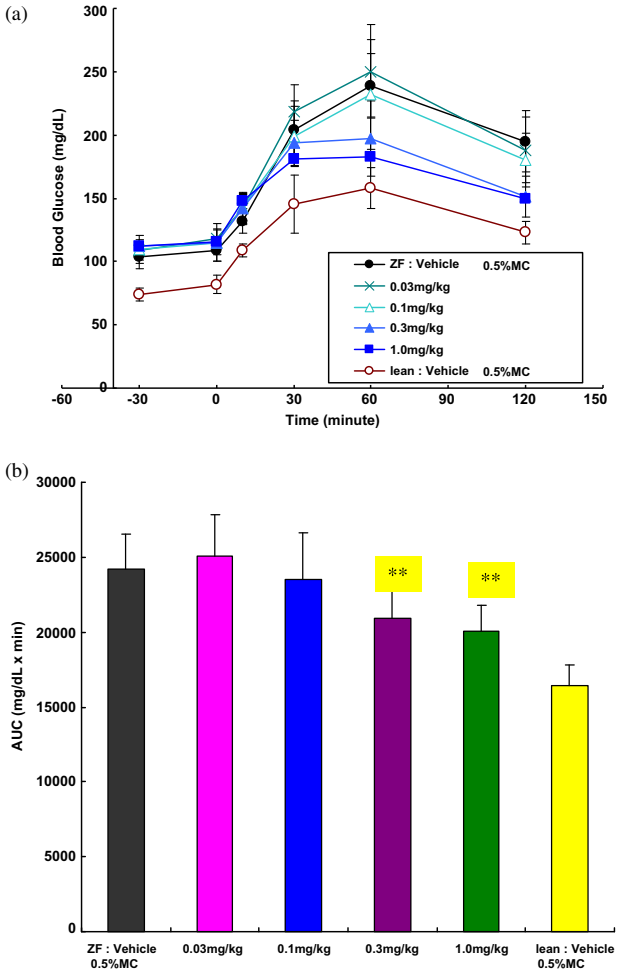

Figure 5. OGTT of **7a** in ZF rats; (a) time course of blood glucose concentration and (b) AUC of blood glucose concentration. Reactive plasma glucose AUC was calculated from 0 to 120 min. All test-compounds in Methyl-Cellulose were administered to ZF rats as a solution with appropriate concentration. Each vertical bar represents the means ±SD (n = 4–9). White circle and yellow bar show the results in lean rat. $^{**}P$ <0.01, Compound **7a**-treated Zucker fatty rats versus vehicle-treated Zucker fatty rats; Dunnett multiple comparison.

kg and 77 ng/mL, respectively), resulting in a close B.A. in these two species. On the other hand, compound **7a** relatively low systemic CL (29 mL/min/kg) and high C_{max} (245 ng/mL) in dogs are believed to contribute to its great B.A. Compound **7a** terminal half-life ($t_{1/2}$) in dogs (15 h) was longer than that in rats (3.3 h), and its distribution volume (V_{dss}) in dogs (10 L/kg) was 1.5-fold higher than that in rats (6.5 L/kg). Considering DPP-4 inhibitory activity and its protein binding ratio (78% for rat, 59% for dog, 69% for monkey, and 73% for human), compound **7a** was expected to show great in vivo efficacy. Next, we evaluated compound **7a** in vivo inhibitory activity for DPP-4 and examined its effect on blood glucose level in oral glucose tolerance test (OGTT) using Zucker-fatty (ZF) rats.

For DPP-4 inhibition experiment, male ZF rats aged 9 weeks were fasted overnight and dosed orally with compound **7a** (1.0 or 3.0 mg/kg). Compound **7a** in vivo inhibitory activity for DPP-4 was then measured against time. As shown in Figure 4, compound **7a** at 3.0 mg/kg produced maximal inhibition of DPP-4 activity 3 h after administration, and its C_{max} was 309 ng/mL with an area under the curve (AUC) of 2167 ng h/mL.

For the OGTT test, male ZF rats aged 10 weeks were fasted overnight and dosed orally with either the vehicle or compound **7a** at different doses (0.03, 0.1, 0.3, and 1.0 mg/kg). Thirty minutes later (t = 0), the rats were orally administrated glucose (2 g/kg), and blood glucose levels were measured against time. As shown in Figure 5, Compound **7a** (0.3 or 1 mg/kg) dose-dependently reduced blood glucose level in ZF rats. Compound **7a** decreased blood glucose level against glucose tolerance and DPP-4 activity in a dose-dependent manner. These findings suggest that the therapeutic effect of **7a** is mediated via increase in GLP-1 level following inhibition of DPP-4.

2.6. Additional profiling of compound 7a

Based on the results described above, compound **7a** was further investigated in safety battery test. For that, it was necessary to determine the final form of **7a**. First, we considered using **7a** as an HCl salt. However, differential scanning calorimetry (DSC) and thermogravimetric analysis (TGA) revealed that the HCl salt form of **7a** is unstable at low temperatures. In fact, the HCl salt form of **7a** generated heat in DSC and showed decrease in weight at around 100 °C in TGA. A wide variety of salts, that is, sulfuric salt, phosphate salt, and methanesulfonic salt were consequently tried, but were found difficult to treat. Finally, a free amine as an anhydrous crystal form was found to be suitable. The free amine form of **7a** was nonhygroscopic under kinetic measurements and dissolved in buffered water (pH 1.2, 5.5, and 6.8) over 1.0 mg/mL.

In toxicology studies, compound **7a** showed no genotoxicity in Ames test and no severe target organ toxicity in 2-week repeated-dose toxicity studies in rats (n = 5, each sex) and monkeys (n = 1, each sex). The No observable adverse effect level (NOAEL) of compound **7a** in these studies was 60 mg/kg/day.

2.7. Conclusion

In summary, we identified in this study 2-({6-[(3*R*)-3-amino-3-methylpiperidine-1-yl]-1,3-dimethyl-2,4-dioxo-1,2,3,4-tetrahy-

dro-5*H*-pyrrolo[3,2-*d*]pyrimidine-5-yl}methyl)-4-fluorobenzonitrile (DSR-12727) (**7a**) as a potent and orally active DPP-4 inhibitor without mechanism-based inactivation of cytochrome P450 3A which is observed in some of other DPP-4 inhibitors. Compound **7a** showed good pharmacokinetics, and dose-dependently reduced blood glucose level in ZF rats. Moreover, compound **7a** exhibited no safety concerns both in vitro and in vivo. It is therefore expected that compound **7a**, as a novel DPP-4 inhibitor, would be useful in the treatment of type 2 diabetes.

3. Experimental section

All reagents and solvents were obtained from commercial suppliers and used without further drying or purification. Other DPP-4 inhibitors were synthesized in our laboratory based on the reported ways. All reactions were performed under nitrogen atmosphere. Normal-phase column chromatography was carried out on a Yamazen W-prep system with pre-packed SiO_2 columns or Amino-SiO_2 columns. Visualization was performed under UV light (254 nm) or ninhydrine. ^{1}H NMR spectra were recorded on Brucker AVANCE 400, and ^{13}C NMR spectra were recorded on Brucker AVANCE 400 set at 100 MHz; all chemical shift (δ) values were referenced to $CDCl_3$ or DMSO as an internal standard and reported as shift (proton count, multiplicity, coupling constant (J)). IR spectra were recorded on a JEOL JIR-SPX60 spectrometer as ATR or KBr Mass spectra (LRMS) were recorded on API 150EX performed by electron spray ionization (ESI) and high-resolution mass spectra (HRMS) were recorded on a Thermo Fischer Scientific LTQ orbitrap Discovery MS equipment. All chemical analyses were performed on a CE Instrument EA1110 and a Yokokawa analytical system IC7000. Test compounds purity was determined by Ultra Fluent Liquid chromatography (UFLC) with Shim-pack XR-ODC 75 mm × 3.0. Purity samples were dissolved in MeOH/0.1% TFA, and the eluent volume was 1.0 mL/min with 10 min-gradient (from 1.0%B to 95%B). Solvent A was H_2O/0.1% TFA and solvent B was CH_3CN/0.1% TFA. Test compounds purity was determined by UFLC and was $\geqslant$95%.

3.1. 1-Benzyl 3-ethyl 3-ethylpiperidine-1,3-dicarboxylate (10b)

The 3-ethyl 3-ethylpiperidin carboxylate **9b** was synthesized as reported in the literature.[19] To a solution of ethyl nipecotate **8** (7.00 g; 44.6 mmol) in THF (10 mL), was added dropwise sodium hexamethyl disilazane (NaHMDS) in THF (1.05 M, 50 ml) at −20 °C to −10 °C, and the resulting solution was stirred for 1 h. EtI (6.95 g; 44.6 mmol) was then added to the solution while keeping the temperature at −10 °C to −20 °C, and the resulting mixture was allowed to warm to room temperature without the cold bath. The reaction mixture was next quenched by H_2O and separated, and the organic layer was dried over Na_2SO_4 and concentrated to afford the intermediate **9b** (8.20 g), which was used in the next reaction without purification. To a solution of **9b** and triethylamine (TEA) (6.75 g) in THF was slowly added carbobenzyloxy chloride (CbzCl) (6.4 ml) at 0 °C, and the resulting mixture was allowed to warm to room temperature with the ice-bath. The reaction mixture was then filtered through Celite, washed with satd NH_4Cl aq and brine, dried over Na_2SO_4, and the filtrate was concentrated. The residue was purified by SiO_2 column chromatography (Hexane/EtOAc = 10/1 to 5/1) to give 7.28 g (51%) of **10b** as a white solid.

^{1}H NMR (400 MHz, $CDCl_3$) δ: 0.82 (3H, bs), 1.18 (3H, br s), 1.40–1.70 (5H, m), 2.04–2.10 (1H, m), 3.10–3.25 (2H, m), 3.60–3.65 (1H, m), 4.00–4.18 (3H, m), 5.12 (2H, s), 7.27–7.40 (5H, m). LRMS (ESI$^+$): *m/z* 414.2.

3.2. Benzyl (3*R*)-3-[(*tert*-butoxycarbonyl)amino]-3-methylpiperidine-1-carboxylate (12a)

To a solution of **9a** (45 g; 263 mmol) and TEA (28.0 g) in THF (270 mL) was slowly added CbzCl (45.2 g; 266 mmol) at 0 °C, and the resulting mixture was allowed to warm to room temperature with the ice-bath and then stirred overnight. The reaction mixture was next filtered through Celite, washed with satd NH_4Cl aq and brine, dried over Na_2SO_4, and the filtrate was concentrated to give **10a** (80.0 g), which was used for the next reaction without purification. A mixture of **10a**, 3 N NaOH aq (150 mL), and MeOH (150 mL) was stirred under reflux for 1 day, and the solvent was removed. The mixture was then extracted by EtOAc under acidic condition, and the organic layer was dried over Na_2SO_4 and concentrated to give the intermediate carboxylic acid **11a** (63.82 g), which was used for the next reaction without purification. To a solution of the carboxylic acid and TEA (24.3 g) in toluene (100 mL) heated to 100 °C was added slowly dropwise DPPA (61.5 g), and the resulting mixture was stirred for 2 h. After cooling to room temperature, the reaction mixture was washed with H_2O, dried over Na_2SO_4, and the filtrate was concentrated to half-volume. To the residue were added *tert*-butyl alcohol (24.4 g) and potassium *tert*-butoxide (2.20 g), and the resulting slurry was stirred for 1 h at 40 °C. The mixture was finally washed with H_2O and brine, dried over Na_2SO_4, and the filtrate was concentrated. The residue was purified by SiO_2 column chromatography (Hexane/EtOAc = 15/1 to 7/1) to give 53.0 g (58%) of **12a** as a white solid.

^{1}H NMR (400 MHz, $CDCl_3$) δ: 1.31 (3H, s), 1.41 (9H, s), 1.20–1.80 (6H, m), 2.80–3.10 (2H, m), 3.80–4.00 (2H, m), 4.40–4.80 (1H, m), 5.00–5.10 (2H, m), 7.28–7.39 (5H, m). LRMS (ESI$^+$): *m/z* 349.3.

Chiral analytical conditions: The column was Chiral-Pack® AD-H, the eluent volume was 0.8 mL/min with Hexane/2-propanol/diethyl amine = 1/5/0.2 (v/v), the temperature was 30 °C and the measuring wavelength was set at 254 nm. Under these conditions **12a** was detected at 8.5 min (>95.0% ee), and the other chiral isomer was detected at 6.8 min.

3.3. Benzyl 3-[(*tert*-butoxycarbonyl)amino]-3-ethylpiperidine-1-carboxylate (12b)

The synthetic route for **12b** was the same as the latter part of the synthesis of **12a**. Starting from **10b** (7.28 g; 22.8 mmol), **12b** (4.23 g; 51%) was obtained as oil. As for the hydroxylation step, the reaction needed 3 days.

^{1}H NMR (400 MHz, $CDCl_3$) δ: 0.84 (3H, bs), 1.41 (9H, s), 1.20–1.80 (6H, m), 2.70–3.05 (2H, m), 3.70–4.10 (2H, m), 5.00–5.30 (2H, m), 7.28–7.39 (5H, m). LRMS (ESI$^+$): *m/z* 363.3.

3.4. *tert*-Butyl [(3*R*)-3-methylpiperidin-3-yl]carbamate (13a)

A mixture of **12a** (10.4 g; 29.9 mmol), 10% Pd/C (50% wet) (1.05 g), and MeOH (60 mL) was stirred at room temperature under H_2 atmosphere for 3 h. The slurry was then filtered through Celite and concentrated, and the residue was purified by Amino-SiO_2 column chromatography ($CHCl_3$/MeOH = 20/1 to 10/1) to give 5.16 g (81%) of **13a** as oil.

^{1}H NMR (400 MHz, $CDCl_3$) δ: 1.32 (3H, s,), 1.44 (9H, s), 1.50–1.60 (1H, m), 1.60–1.75 (1H, m), 2.22 (1H, m), 2.50–2.70 (3H, m), 3.00–3.18 (2H, m), 5.09 (1H, bs). LRMS (ESI$^+$): *m/z* 215.4.

3.5. *tert*-Butyl (3-ethylpiperidin-3-yl)carbamate (13b)

The synthetic route for **13b** was the same as that for **13a**. Starting from **12b** (4.23 g; 11.7 mmol), **13b** (2.65 g; 99%) was obtained as oil.

^{1}H NMR (400 MHz, $CDCl_3$) δ: 0.81 (3H, t, J = 7.5 Hz), 1.22 (1H, dt, J = 13.6, 4.2 Hz), 1.43 (9H, s), 1.40–1.71 (2H, m), 1.87 (1H, br s), 2.11 (1H, s), 2.27 (1H, s), 2.41 (1H, d, J = 12.2 Hz), 2.55 (1H, dt. J = 11.6, 3.0 Hz), 3.00 (2H, dd, J = 30, 12.1 Hz), 4.85 (1H, bs). LRMS (ESI$^+$): m/z 229.4.

3.6. 4-*tert*-Butyl 2-ethyl 3-amino-1-(2-bromo-5-fluorobenzyl)-5-{(3*R*)-3-[(*tert*-butoxycarbonyl)amino]-3-methylpiperidin-1-yl}-1*H*-pyrrole-2,4-dicarboxylate (15a)

A mixture of **14** (5.00 g; 20.4 mmol) and **13a** (4.37 g; 20.4 mmol) in CH_3CN (60 ml) was stirred at 50 °C for 1 h. After cooling to room temperature, 1,8-diazabicyclo[5,4,0]undeca-7-ene (DBU) (6.20 g; 40 mmol) and 2-bromo-5-fluoro-benzylamine (4.99 g; 24.4 mmol) were added to the mixture, and the resulting mixture was stirred at 80 °C for 10 h. After removal of the solvent, the residue was diluted with EtOAc, and washed with H_2O, 10%$KHSO_4$ aq, 10%NaOH aq and brine. The EtOAc layer was dried over Na_2SO_4 and the filtrate was concentrated.

The residue was dissolved in DMF (60 mL), and ethyl bromoacetate (2.80 mL; 28 mmol) and K_2CO_3 (8.5 g) were added. The resulting slurry was then stirred at 50 °C for 2 h and cooled to room temperature. The slurry was diluted with EtOAc, filtered through Celite, and washed with satd NH_4Cl aq and brine. The organic layer was dried over Na_2SO_4, and the filtrate was concentrated.

To *tert*-butyl alcohol (30 mL) was added lithium amide (1.16 g; 48 mmol). After stirring at 80 °C for 1 h, the resulting mixture was cooled to 30 °C, and CH_3CN (40 mL) was added. A solution of the alkylated product from the third step in toluene (10 mL) was next added dropwise, and the reaction mixture was stirred for 2 h at 30 °C. The solvent was removed, and to the residue was added EtOAc. The resulting mixture was finally washed with satd NH_4Cl aq and brine, the organic layer was dried over Na_2SO_4, and the filtrate was concentrated. The residue was purified by SiO_2 column chromatography (Hexane/EtOAc = 6/1 to 3/1) to give 5.80 g (44% from **14**) of **15a** as amorphous solid. In addition to the target product **15a**, the ester exchange product (R_2 = *tert*-butyl) was also obtained as an amorphous (415 mg).

^{1}H NMR (400 MHz, $CDCl_3$) δ: 1.13 (3H, t, J = 7.1 Hz), 1.26 (3H, s), 1.39 (9H, s), 1.40–1.60 (3H, m), 1.63 (9H, s), 2.10–2.40 (1H, m), 2.50–2.9 (2H, m), 3.10 (1H, s), 3.40 (1H, m), 4.17 (2H, q, J = 7.1 Hz), 5.30–5.60 (2H, m), 6.21 (1H, d, J = 9.0 Hz), 6.86 (1H, td, J = 8.3, 2.8 Hz), 7.51 (1H, dd, J = 8.7, 3.6 Hz). LRMS (ESI$^+$): m/z 653.5, 655.5.

3.7. *tert*-Butyl 5-(2-bromo-5-fluorobenzyl)-6-{(3*R*)-3-[(*tert*-butoxycarbonyl)amino]-3-methylpiperidin-1-yl}-1,3-dimethyl-2,4-dioxo-2,3,4,5-tetrahydro-1*H*-pyrrolo[3,2-*d*]pyrimidine-7-carboxylate (16a)

To a solution of **15a** (784 mg; 1.6 mmol) and ester exchange product (42 mg) in AcOH (15 mL) was added dropwise KOCN (0.20 g; 2.5 mmol) in H_2O (0.40 g) at 40 °C. After stirring for 2 h, the resulting mixture was diluted with EtOAc and washed with H_2O, 20% $NaHCO_3$ aq and brine. The organic layer was then dried over Na_2SO_4, and the filtrate was concentrated. The residue was used for the next reaction without further purification. A mixture of the residue, K_2CO_3 (340 mg; 2.2 mmol), and DMF (10 mL) was stirred at 50 °C for 5 h, and then cooled to 30 °C. To the slurry was added additional K_2CO_3 (340 mg; 2.2 mmol), and then methyl iodide (0.20 mL; 3.2 mmol) was added dropwise. After stirring for 5 h, H_2O (excess) was added to the mixture, and the precipitate was collected by filtration. The white solid was slurred in 2-propanol at 60 °C for 2 h, filtered, and dried to afford 550 mg (51%) of **16a** as a white solid.

^{1}H NMR (400 MHz, $CDCl_3$) δ: 1.25 (3H, s), 1.40 (9H, s), 1.61 (9H, s), 1.50–1.65 (3H, m), 2.10 (1H, br s), 2.72 (1H, br s), 2.80–2.92 (1H, m), 2.99–3.12 (2H, m), 3.36 (3H, s), 3.59 (3H, s), 4.54 (1H, br s), 6.16 (1H, d, J = 7.6 Hz), 6.86 (1H, td, J = 8.4, 3.0 Hz), 7.53 (1H, q, J = 8.7, 5.2 Hz). LRMS (ESI$^+$): m/z 678.5, 680.5.

3.8. *tert*-Butyl 6-{(3*R*)-3-[(tert-butoxycarbonyl)amino]-3-methylpiperidin-1-yl}-5-(2-cyano-5-fluorobenzyl)-1,3-dimethyl-2,4-dioxo-2,3,4,5-tetrahydro-1*H*-pyrrolo[3,2-*d*]pyrimidine-7-carboxylate (17a)

A mixture of **16a** (204 mg; 0.3 mmol), Pd(t-Bu_3P)$_2$ (15 mg; 0.03 mmol), zinc cyanide (22 mg; 0.18 mmol), and *N*-methyl pyrrolidone (NMP) (3.0 mL) was air-vacuated, flushed with N_2, and then stirred for 1 h at 100 °C. After cooling to room temperature, the reaction mixture was filtered through Celite, and NH_4OH-satd NH_4Cl aq-H_2O (4/4/1, (v/v)) was added with vigorous stirring. The formed light-yellow solid was collected by filtration, and stirred in CH_3CN at 80 °C for 2 h, then at 0 °C for 1 h, and finally filtered to give a crude compound. The crude compound was purified by SiO_2 column chromatography ($CHCl_3$/CH_3CN = 15/1 to 5/1) to give 102 mg (54%) of **17a** as a white solid.

^{1}H NMR (400 MHz, $CDCl_3$) δ: 1.25 (3H, s), 1.39 (9H, s), 1.62 (9H, s), 1.50–1.65 (3H, m), 2.10 (1H, br s), 2.72 (1H, br s), 2.80–2.92 (1H, m), 3.05–3.12 (2H, m), 3.34 (3H, s), 3.58 (3H, s), 4.48 (1H, br s), 6.35(1H, d, J = 7.4 Hz), 7.05 (1H, td, J = 8.3, 2.6 Hz), 7.71 (1H, dd, J = 8.5, 5.2 Hz). LRMS (ESI$^+$): m/z 625.5.

3.9. 2-({6-[(3*R*)-3-amino-3-methylpiperidine-1-yl]-1,3-dimethyl-2,4-dioxo-1,2,3,4-tetrahydro-5*H*-pyrrolo[3,2-*d*]pyrimidine-5-yl}methyl)-4-fluorobenzonitrile (7a)

To a asolution of intermediate **17a** (102 mg; 0.17 mmol) in CH_3CN (20 mL), was added dropwise a solution of $PhSO_3H$ monohydrate (58 mg; 0.33 mmol) in EtOH (5.0 mL) at 40 °C, and the resulting mixture was stirred at 80 °C for 2 h. After cooling to room temperature, the reaction mixture was diluted with EtOAc, and 2 N NaOH aq was added to adjust the pH between 8 and 10. The mixture was then separated, and the H_2O layer was washed twice with EtOAc. The collected organic layer was washed with brine, dried over Na_2SO_4, and the filtrate was concentrated. The residue was purified by Amino-SiO_2 column chromatography ($CHCl_3$/MeOH = 20/1 to 10/1) to give 70 mg (94%) of **7a** as a white solid.

Chiral analytical conditions: The column was Chiral-Pack® AD-H. The eluent volume was 0.8 mL/min with Hexane/2-propanol/diethyl amine = 80/20/0.2 (v/v), the temperature was 25 °C and the measured wavelength was at 291 nm. Under these conditions **7a** was detected at 24.8 min (>99.0% ee), and the other enantiomer was detected at 29.5 min (>97% ee).

^{1}H NMR (400 MHz, DMSO) δ: 0.89 (3H, s), 1.28–1.60 (5H, m), 1.61–1.71 (1H, m), 2.59 (2H, q, J = 11.2, 10.3 Hz), 2.70–2.83 (2H, m), 3.14 (3H, s), 3.38 (3H, s), 5.65 (2H, s), 6.00 (1H, s), 6.34 (1H, dd, J = 9.6, 2.5 Hz), 7.33 (1H, td, J = 8.5, 2.6 Hz), 7.99 (1H, q, J = 8.6, 5.5 Hz). ^{13}C NMR (100 MHz, $CDCl_3$) δ: 22.1, 27.2, 27.71, 31.8, 37.9, 45.5, 48.2, 54.0, 65.4, 84.7, 106.05, 106.1 (^4J(C,F) = 3.3 Hz), 114 (^2J(C,F) = 24.0 Hz), 115.3 (^2J(C,F) = 22.7 Hz), 116.4, 135.1 (^3J(C,F) = 9.5 Hz), 136.3, 146.3 (^3J(C,F) = 8.5 Hz), 151.5, 151.7, 155.2, 165.4 (^1J(C,F) = 255 Hz). IR (KBr): 2939, 2223, 1689, 1640 cm^{-1}. HRMS (ESI$^+$): m/z 425.2082 (Calcd m/z 425.2096 for $C_{22}H_{25}FN_6O_2$ +H). Anal. Calcd for $C_{22}H_{25}FN_6O_2$: C, 62.25; H, 5.94; N, 19.80; F, 4.48. Found: C, 61.94; H, 5.86; N, 19.81; F, 4.34. mp 176–179 °C (IPA/H_2O). $[\alpha]_D^{25}$ −9.5 (c 0.93, EtOH/H_2O (95:5, v/v)).

3.10. 4-*tert*-Butyl 2-ehtyl 3-amino-1-(2-bromo-5-fluorobenzyl)-5-{3-[(*tert*-butoxycarbonyl)amino]-3-ethylpiperidin-1-yl}-1*H*-pyrrole-2,4-dicarboxylate (15b)

The synthetic route for **15b** was the same as that for **15a**. The target compound **15b** (2.52 g: 34%) was obtained from **14** (2.69 g; 11 mmol).

^{1}H NMR (400 MHz, $CDCl_3$) δ: 0.76 (3H, br s), 1.20–1.30 (1H, m), 1.40 (9H, s), 1.40–1.70 (2H, m), 1.62 (9H, s), 1.88 (2H, m), 2.80–3.50 (5H, m), 4.17 (2H, q, J = 7.1 Hz), 5.30–5.60 (2H, m), 6.25 (1H, d, J = 7.2 Hz), 6.86 (1H, td, J = 8.4, 3.0 Hz), 7.52 (1H, dd, J = 8.7, 5.2 Hz). LRMS (ESI$^+$): m/z 667.5, 669.5.

3.11. *tert*-Butyl 5-(2-bromo-5-fluorobenzyl)-6-{3-[(*tert*-butoxycarbonyl)amino]-3-ethylpiperidin-1-yl}-1,3-dimethyl-2,4-dioxo-2,3,4,5-tetrahydro-1*H*-pyrrolo[3,2-*d*]pyrimidine-7-carboxylate (16b)

The synthetic route for **16b** was almost the same as that for **16a**. The target compound **16b** (1.60 g; 68%) was obtained from **15b** (2.30 g; 3.4 mmol). Purification was carried out using SiO_2 column chromatgraphy (Hexane/EtOAc = 3/1 to 1/1).

^{1}H NMR (400 MHz, $CDCl_3$) δ: 0.73 (3H, s), 1.40 (9H, s), 1.61 (9H, s), 1.40–1.65 (3H, m), 1.73–1.82 (1H, m), 2.60–3.00 (3H, m), 3.10–3.20 (1H, m), 3.35 (3H, s), 3.59 (3H, s), 4.42 (1H, br s), 5.59 (2H, m), 6.19 (1H, d, J = 7.9 Hz), 6.85 (1H, td, J = 8.3, 3.0 Hz), 7.53 (1H, dd, J = 8.8, 5.2 Hz). LRMS (ESI$^+$): m/z 692.7, 694.7.

3.12. *tert*-Butyl 6-{3-[(*tert*-butoxycarbonyl)amino]-3-ethylpiperidin-1-yl}-5-(2-cyano-5-fluorobenzyl)-1,3-dimethyl-2,4-dioxo-2,3,4,5-tetrahydro-1*H*-pyrrolo[3,2-*d*]pyrimidine-7-carboxylate (17b)

The synthetic route for **17b** was almost the same as that for **17a**. The target compound **17b** (1.00 g; 68%) was obtained from **16b** (1.60 g; 2.3 mmol). Purification was carried out using SiO_2 column chromatography (Hexane/EtOAc = 3/1 to 1/1), and was followed by recrystallization from CH_3CN.

^{1}H NMR (400 MHz, $CDCl_3$) δ: 0.74 (3H, s), 1.39 (9H, s), 1.61 (9H, s), 1.50–1.62 (3H, m), 1.65–1.80 (2H, m), 2.80–2.92 (1H, m), 2.99–3.12 (2H, m), 3.34 (3H, s), 3.58 (3H, s), 4.34 (1H, br s), 5.79 (2H, s), 6.38 (1H, d, J = 9.1 Hz), 7.06 (1H, td, J = 8.2, 2.5 Hz), 7.71 (1H, dd, J = 8.6, 5.3 Hz). LRMS (ESI$^+$): m/z 639.8

3.13. 2-({6-[(3*R*)-3-Amino-3-ethylpiperidin-1-yl]-1,3-dimethyl-2,4-dioxo-1,2,3,4-tetrahydro-5*H*-pyrrolo[3,2-*d*]pyrimidine-5-yl}methyl)-4-fluorobenzonitrile ((+)-7b)

See Section 3.14

3.14. 2-({6-[(3S)-3-amino-3-ethylpiperidin-1-yl]-1,3-dimethyl-2,4-dioxo-1,2,3,4-tetrahydro-5H-pyrrolo[3,2-*d*]pyrimidine-5-yl}methyl)-4-fluorobenzonitrile ((-)-7b)

The synthetic route for **7b** was the same as that for **7a**. The target compound *rac*-**7b** (0.70 g; 99%) was obtained from **17b** (1.00 g; 1.6 mmol).

The racemic compound *rac*-**7b** (563 mg) was separated to each enantiomer by chiral HPLC column resolution at Daicel Co. Ltd, to afford (+)-**7b** (250 mg) and (−)-**7b** (220 mg) as amorphous solid.

Chiral analytical conditions: The column was Chiral-Pack® AD-H. The eluent volume was 1.0 mL/min with Hexane/2-propanol/diethyl amine = 70/30/0.1 (v/v), the temperature was 40 °C and the measured wavelength was at 264 nm. Under these conditions (+)-**7b** was detected at 9.2 min (>97.0% ee), and (−)-**7b** was detected at 7.8 min (>99.0% ee).

$[\alpha]_D^{25}$ +6.62 (c 1.27, EtOH/H_2O (95:5, v/v)) for (+)-**7b**, and $[\alpha]_D^{25}$ −5.85 (c 1.27, EtOH/H_2O (95:5, v/v)) for (−)-**7b**.

^{1}H NMR (400 MHz, DMSO) δ: 0.64 (1H, t, J = 7.5 Hz), 1.10–1.20 (1H, m), 1.20–1.40 (5H, m), 1.48–1.59 (1H, m), 1.62–1.73 (1H, m), 2.57 (2H, t, J = 12.1 Hz), 2.70–2.80 (1H, m), 2.80–2.90 (1H, m), 3.14 (3H, s), 3.38 (3H, s), 5.65 (2H, dd, J = 17.0, 9.8 Hz), 6.00 (1H, s), 6.40 (1H, dd, J = 9.6, 2.5 Hz), 7.33 (1H, td, J = 8.5, 2.6 Hz), 8.00 (1H, dd, J = 8.6, 5.4 Hz). ^{13}C NMR (100 MHz, $CDCl_3$) δ: 6.9, 21.6, 27.8, 31.8, 34.7, 45.6, 51.3, 54.1, 54.3, 62.8, 84.7, 85.5, 106.15, 106.2 (^4J(C,F) = 3.3 Hz), 114.0 (^2J(C,F) = 23.9 Hz), 115.4 (^2J(C,F) = 22.8 Hz), 116.4, 135.2 (^3J(C,F) = 9.5 Hz), 136.3, 146.4 (^3J(C,F) = 8.5 Hz), 151.5, 151.6, 155.2, 165.5 (^1J(C,F) = 255 Hz). IR (ATR): 2935, 2802, 2223, 1699, 1643 cm^{-1}. HRMS (ESI$^+$): m/z 439.2241 (Calcd m/z 439.2252 for $C_{23}H_{27}FN_6O_2$ +H). Anal. Calcd for $C_{23}H_{27}FN_6O_2$: C, 63.00; H, 6.21; N, 19.17. Found: C, 62.68; H, 6.23; N, 18.99.

3.15. 4-*tert*-Butyl 2-ehtyl 3-amino-1-(2-bromo-5-fluorobenzyl)-5-{(3*R*)-3-[(*tert*-butoxycarbonyl)amino]piperidin-1-yl}-1*H*-pyrrole-2,4-dicarboxylate (15c)

The synthetic route for **15c** was the same as that for **15a**. The target compound **15c** (279 mg; 44%) was obtained from **14** (245 mg; 1.0 mmol) and *tert*-butyl [(*R*)-3-piperidine-3-yl]carbamate (200 mg; 1.0 mmol).

^{1}H NMR (400 MHz, $CDCl_3$) δ: 1.12 (3H, br s), 1.40 (9H, s), 1.30–1.41 (1H, m), 1.50–1.61 (2H, m), 1.60 (9H, s), 1.70–1.81 (1H, m), 1.88–1.92 (1H, m), 2.50 (1H, m), 2.90–3.30 (2H, m), 3.51-3.80 (1H, m), 4.11 (2H, q, J = 7.1 Hz), 5.40–5.60 (2H, m), 6.23 (1H, d, J = 7.2 Hz), 6.81 (1H, m), 7.50 (1H, m). LRMS (ESI$^+$): m/z 639.5, 641.5.

3.16. *tert*-Butyl 5-(2-bromo-5-fluorobenzyl)-6-{(3R)-3-[(*tert*-butoxycarbonyl)amino]piperidin-1-yl}-1,3-dimethyl-2,4-dioxo-2,3,4,5-tetrahydro-1*H*-pyrrolo[3,2-*d*]pyrimidine-7-carboxylate (16c)

The synthetic route for **16c** was almost the same as that for **16a**. The target compound **16c** (175 mg; 66%) was obtained from **15c** (263 mg; 0.40 mmol). Purification was carried out using SiO_2 column chromatgraphy (Hexane/EtOAc = 3/1 to 1/1).

^{1}H NMR (400 MHz, $CDCl_3$) δ: 1.39 (9H, s), 1.30–1.40 (2H, m), 1.59 (9H, s), 1.50–1.60 (1H, m), 1.73–1.82 (1H, m), 2.70–3.00 (3H, m), 3.24 (1H, br s), 3.34 (3H, s), 3.57 (3H, s), 3.50–3.80 (1H, m), 4.66 (1H, br s), 5.50–5.80 (2H, m), 6.14 (1H, d, J = 7.9 Hz), 6.83 (1H, td, J = 8.3, 3.0 Hz), 7.52 (1H, dd, J = 8.8, 5.2 Hz). LRMS (ESI$^+$): m/z 664.7, 666.7.

3.17. *tert*-Butyl-6-{(3R)-3-[(*tert*-butoxycarbonyl)amino]piperidin-1-yl}-5-(2-cyano-5-fluorobenzyl)-1,3-dimethyl-2,4-dioxo-2,3,4,5-tetrahydro-1*H*-pyrrolo[3,2-*d*]pyrimidine-7-carboxylate (17c)

The synthetic route for **17c** was almost the same as that for **17a**. The target compound **17c** (89 mg; 56%) was obtained from **16c** (175 mg; 0.26 mmol). Purification was carried out using SiO_2 column chromatography (Hexane/EtOAc = 3/1 to 1/1).

^{1}H NMR (400 MHz, $CDCl_3$) δ: 1.38 (9H, s), 1.35–1.41 (1H, m), 1.60 (9H, s), 1.50–1.80 (3H, m), 2.70–3.00 (3H, m), 3.16 (1H, br s), 3.34 (3H, s), 3.55 (3H, s), 3.40–3.70 (1H, m), 4.50 (1H, br s), 5.79 (2H, s), 6.39 (1H, d, J = 9.1 Hz), 7.03 (1H, td, J = 8.2, 2.5 Hz), 7.71 (1H, dd, J = 8.6, 5.3 Hz). LRMS (ESI$^+$): m/z 611.8.

3.18. 2-({6-[(3*R*)-3-Amino-piperidin-1-yl]-1,3-dimethyl-2,4-dioxo-1,2,3,4-tetrahydro-5*H*-pyrrolo[3,2-*d*]pyrimidine-5-yl}methyl)-4-fluorobenzonitrile HCl salt (6)

The synthetic route for **6** was the same as that for **7a**. The free amine form of compound **6** (58 mg; quant) was obtained from **17c** (89 mg; 0.14 mmol).

After purification using Amino-SiO_2 column chromatography, the free amine was dissolved in MeOH (2.0 mL). To the resulting solution was added 1.0 N HCl aq (0.2 mL), and the mixture was concentrated, co-evaporated with water three times, and dried to give 62 mg (quant) of **6** as an amorphous solid.

^{1}H NMR (400 MHz, DMSO) δ: 1.50–1.60 (2H, m), 1.75–2.00 (2H, m), 2.70–2.80 (1H, m), 2.81–2.90 (2H, m), 3.12 (3H, s), 3.20–3.40 (2H, m), 3.39 (3H, s), 5.59 (2H, s), 6.12 (1H, s), 6.40 (1H, dd, J = 9.4, 2.4 Hz), 7.33 (1H, td, J = 8.5, 2.5 Hz), 7.99 (1H, dd, J = 8.6, 5.5 Hz), 8.05–8.20 (3H, m). ^{13}C NMR (100 MHz, DMSO) δ: 22.1, 27.1, 27.5, 31.9, 45.3, 46.5, 53.2, 54.7, 86.0, 105.3, 106.3 (^4J(C,F) = 2.8 Hz), 113.8 (^2J(C,F) = 23.8 Hz), 115.7 (^2J(C,F) = 22.6 Hz), 116.8, 136.1, 136.2, 136.4, 146.5 (^3J(C,F) = 8.5 Hz), 150.8, 151.0, 154.6, 164.9 (^1J(C,F) = 252 Hz). IR (ATR): 2946, 2225, 1685, 1633 cm^{-1}. HRMS (ESI$^+$): *m/z* 411.1929 (Calcd *m/z* 411.1939 for $C_{21}H_{23}FN_6O_2$ +H). Anal. Calcd for $C_{21}H_{23}FN_6O_2$ HCl 1.25H_2O: C, 53.73; H, 5.69; N, 17.90; Cl, 7.55. Found: C, 53.56; H, 5.63; N, 17.95; Cl, 7.47.

3.19. Measurement of DPP-4 inhibition rate

DPP-4 activity in plasma samples was measured using Glycyl-L-Proline 4-Methylcoumaryl-7-Amide (Gly-Pro-MCA) as substrate. Relative fluorescence units (RFUs) of 7-amino-4-methylcoumarin (AMC) liberated from Gly-Pro-MCA by DPP-4 in plasma were measured to determine the amount of cleaved substrate, and DPP-4 activity was calculated from this measurement (1 U = 1 μmol substrate cleavage/min). DPP-4 concentration in human blood plasma was adjusted to 10% and used as source of enzyme with the concentration of each compound. The final concentration was adjusted to 50 μL by addition of the substrate Gly-Pro-MCA. Fluorescence intensity in RFUs (excitation wavelength 380 nm/emission wavelength 460 nm) was continuously monitored by a fluorescence plate reader at room temperature (excitation at 380 nm, measurement at 460 nm) to determine enzymatic activity. The concentration of each test-compound that inhibited enzymatic activity by 50% was determined as IC_{50}.

3.20. Estimation of MBI parameters

A mixture of human liver microsomes and appropriate dilutions of test-compound (0, 1, and 10 μL) was pre-incubated for 15 min at 37 °C with or without NADPH. The mixture was next diluted 20-fold with assay buffer containing midazolam, a probe substrate of CYP3A, and NADPH, incubated for an additional 5 min at 37 °C, and quenched in three-fold the amount of MeOH to completely stop the reaction. The amount of midazolam metabolite, which was in the form of 1-hydroxy midazolam, was measured by LC/MS/MS to determine the remaining CYP3A activity. The decrease in activity with and without NADPH was divided by time (15 min) to give k_{obs}, which in turn provided the concentration of the inactivator [I] in Eq. (1), k_{inact} and K_I, and subsequently allowed determination of MBI.

3.21. PK/PD test procedure

Zucker fatty rats (male, 9 weeks old) were fasted for 24 h starting from removal of food until the start of pre-dose blood sampling (−0.5 h), and kept fasted until the end of blood sampling performed 12 h after dosing. The rats received the test-compound (substance) solution orally by gavage. Blood samples were collected 0.5 h before (−0.5 h), and at 0.25, 0.5, 1, 2, 4, 6, 8, 10, 12, 16, and 24 h after dosing (0 h). The time-course of plasma concentration and change in plasma DPP-4 activity after administration of **7a** (1.0, 3.0 mg/kg) were determined. DPP-4 activity in plasma samples was measured in the same manner as that for measurement of DPP-4 inhibition rate. Plasma dilution buffer (5 μL containing 80 mmol/L $MgCl_2$, 140 mmol/L NaCl, 25 mmol/L HEPES, 1% (w/v%) BSA, pH 7.8) was placed into each well of a 96-well plate and a 96 well Half Area Black with Clear Flat Bottom 3881 (Corning Incorporated), and 5 μL of each plasma sample or distilled water (for measurement of background reaction) was added to individual wells, mixed and left to stand for at least 5 min. To initiate the reaction, 10 μL of 100 μmol/L Gly-Pro-MCA solution diluted with substrate dilution buffer (140 mmol/L NaCl, 25 mmol/L HEPES, 1% (w/v%) BSA, pH 7.8) was added to each well containing a plasma sample or distilled water. Two minutes later, fluorescence intensity in RFUs (excitation wavelength 380 nm/emission wavelength 460 nm) was continuously monitored for 3 min at 30 s-intervals using a fluorescence microplate reader (SpectraMax® Gemini EM). Next, 20 μL of standard AMC solution (1.28, 2.52, 5, 10, 20, and 40 μmol/L; diluted with plasma dilution buffer, substrate dilution buffer, rat plasma and DMSO) was placed into each of the wells with no plasma samples or distilled water, and fluorescence intensity in RFUs (excitation wavelength 380 nm/emission wavelength 460 nm) of the standard AMC solution was measured to construct a calibration curve of RFU against AMC per well. The curve was constructed on an arithmetic scale using unweighted linear regression implemented in software, SoftMax®Pro version 4.3.1 (Molecular Devices Corporation), within the fluorescence microplate reader. The rates of AMC production in the samples and background wells were calculated using the calibration curve. The net rate of AMC production (nmol/min) in a given sample well was determined by subtracting mean background rate from the rate for the sample well. DPP-4 activity (mU/mL) per plasma unit was calculated by dividing the rate of AMC production by the volume of plasma sample used for the measurement. Duplicate measurements were performed for standard AMC solution and for plasma samples.

3.22. OGTT test procedure

Zucker fatty rats (male, 10 weeks) and Zucker lean rats (male, 10 weeks old) described as lean in Figure 5 were fasted for 24 h starting from the day before each OGTT. Glucose (0.2 g/mL D-glucose solution) was orally loaded by gavage in a volume of 10 mL/kg (2 g of D-glucose/kg). Each concentration of **7a** (0.03, 0.1, 0.3, and 1.0 mg/kg) suspension or 0.5% Methyl Cellulose (MC) solution used as a control was administered once 30 min prior to glucose loading. Blood samples were taken just before administration of test-substance or 0.5% MC solution (−30 min relative to the time of glucose loading), just before glucose loading (taken as 0 min), and 10, 30, 60, and 120 min after glucose loading for determination of blood glucose concentration. Blood glucose concentration was measured for all blood collection time points. A 10 μL blood sample taken from the tail vein of each rat was immediately mixed with 100 μL of 0.62 mol/L perchloric acid solution. Potassium carbonate solution (50 μL, 0.37 mol/L) was then added and mixed. The deproteinized samples were stored in a refrigerator set at 4 °C until measurement of blood glucose concentration. Blood glucose concentration was measured using a commercially available kit, Glucose CII test Wako (Wako Pure Chemical Industries, Ltd). The deproteinized samples were centrifuged at 2,000 rpm for 10 min, and 15 μL of the supernatant of each test sample and glucose

standard solutions (100, 250, 500, and 750 mg/dL) were added to 96-well plates, followed by addition of 200 μL of coloring reagent to each well and mixing. Color reaction was allowed to develop for 18–35 min at room temperature and absorbance was measured using a microplate reader (SpectraMax®190) at a main wavelength of 505 nm and a sub-wavelength of 700 nm. A linear calibration curve was constructed from absorbance differences ($A_{505} - A_{700}$, *Y*-axis) of glucose standard solutions (mg/dL, *X*-axis), using a software provided with the microplate reader (SoftMax®Pro version 4.3.1). Glucose concentration of each test sample was determined by interpolation of its absorbance difference ($A_{505} - A_{700}$) on the standard curve. Each sample and standard solutions were determined in duplicate.

Acknowledgments

We are thankful to Mr. H. Hochigai for providing compound 6, Mr. S. Suetsugu for making the metabolite of compounds, K. Bando for performing the elemental analysis, and Ms. I. Taoka for recording MS spectra.

Supplementary data

Supplementary data associated with this article can be found, in the online version, at doi:10.1016/j.bmc.2011.07.042.

References and notes

1. Colberg, S. R. *ACSM'S Health Fitness J.* **2008**, *12*, 16. For latest information, please see the website of World Health Organization at http://www.who.int/diabetes/facts/world_figures/en/.
2. For a review, see: (a) Mizuno, C. S.; Chittiboyina, A. G.; Kurtz, T. W.; Pershadsingh, H. A.; Avery, M. A. *Curr. Med. Chem.* **2008**, *15*, 61; (b) Barnett, A. H. *Br. J. Diab. Vasc. Dis.* **2008**, *8*, 45.
3. For some references, see: (a) Holst, J. J. *Diabetologia* **2006**, *49*, 253; (b) Knudsen, L. B. *J. Med. Chem.* **2004**, *47*, 4128.
4. (a) Mentlein, R.; Gallwitz, B.; Schmidt, W. E. *J. Eur. Biochem.* **1993**, *214*, 829; (b) Kieffer, T. J.; McIntosh, C. H.; Pederson, T. A. *Endocrinology* **1995**, *136*, 3585; (c) Holst, J. J.; Deacon, C. F. *Diabetologia* **2005**, *48*, 612; For reviews, see: (d) Deacon, C. F. *Horm. Metab. Res.* **2004**, *36*, 761.
5. Farilla, L.; Hui, H.; Bertolotto, C.; Kang, E.; Bulotta, A.; Di Mario, U.; Perfetti, R. *Endocrinology* **2002**, *143*, 4397.
6. Reimer, M. K.; Holst, J. J.; Ahren, B. *Eur. J. Endocrinol.* **2002**, *146*, 717.
7. Pospisilik, A.; Martin, J.; Doty, T.; Ehses, J. A.; Pamir, N.; Lynn, F. C.; Piteau, S.; Demuth, H. –U.; McIntosh, C. H. S.; Pederson, R. A. *Diabetes* **2003**, *52*, 741.
8. For a review, see: Havale, S. H.; Manojit, Pal *Bioorg. Med. Chem.* **2009**, *17*, 1783.
9. (a) Kim, D.; Wang, L.; Beconi, M.; Eiermann, G. J.; Fisher, M. H.; He, H.; Hickey, G. J.; Kowalchick, J. E.; Leiting, B.; Lynos, K.; Marsilio, F.; McCann, M. E.; Patel, R. A.; Petrov, A.; Scapin, G.; Patel, S. B.; Roy, R. S.; Wu, J. K.; Wyvratt, M. J.; Zhang, B. B.; Zhu, L.; Thronberry, N. A.; Weber, A. E. *J. Med. Chem.* **2005**, *48*, 141; (b) Miller, S. A.; St. Onge, E. L. *Ann. Pharmcother.* **2006**, *40*, 1336.
10. Villhauer, E. B.; Brinkman, J. A.; Naderi, G. B.; Burkey, B. F.; Dunning, B. E.; Prasad, K.; Mangold, B. L.; Russell, M. E.; Hughes, T. E. *J. Med. Chem.* **2003**, *46*, 2774.
11. Augeri, D. J.; Robl, J. A.; Betebenner, D. A.; Magnin, D. R.; Khanna, A.; Robertson, J. G.; Wang, A.; Simpkins, L. M.; Taunk, P.; Huang, Q.; Han, S.-P.; Abboa-Offei, B.; Cap, M.; Xin, L.; Tao, L.; Tozzo, E.; Welzel, G. E.; Egan, D. M.; Marcinkeviciene, J.; Chang, S. Y.; Biller, S. A.; Kirby, M. S.; Parker, R. A.; Hamann, L. G. *J. Med. Chem.* **2005**, *48*, 5025.
12. (a) Gwaltney, S. L.; Aertgeerts, K.; Feng, J.; Kaldor, S. W.; Kassel, D. B.; Manuel, M.; Navre, M.; Prasad, G. S.; Shi, L.; Skene, R. J.; Stafford, J. A.; Wallace, M.; Wu, R.; Ye, S.; Zhang, Z. *Abstaracts of Papers*, 231st, Meeting of the American Chemical Society, Atlanta, GA, 2006; American Chemical Society: Washington, DC, 2006; MEDI-018.; (b) Feng, J.; Zhang, Z.; Wallace, M. B.; Sttaford, J. A.; Kaldor, S. W.; Kassel, D. B.; Navre, M.; Shi, L.; Skene, R. J.; Asakawa, T.; Takeuchi, K.; Xu, R.; Webb, D. R.; Gwaltney, S. L. *J. Med. Chem.* **2007**, *50*, 2297.
13. Eckhardt, M.; Langkopf, E.; Mark, M.; Tadayyon, M.; Thomas, L.; Nar, H.; Pfrengle, W.; Guth, B.; Lotz, R.; Sieger, P.; Fuchs, H.; Himmelsbach, F. *J. Med. Chem.* **2007**, *50*, 6450.
14. (a) Nakahira, H.; Hochigai, H. World Patent 2004048379, 2004; (b) Nakahira, H.; Hochigai, H; Takeda, T.; Kobayashi, T.; W. Ewan Hume. World Patent 2005021550, 2005; (c) Nakahira, H.; Hochigai, H.; Uchiyama, K.; World Patent 2006030847, 2006; (d) Nakahira, H.; Kimura, H.; Hochigai, H. World Patent 2006068163, 2006; (e) Nakahira, H.; Kimura, H.; Hochigai, H. World Patent 2006112331, 2006
15. For a review, see: Kalgutkar, A. S.; Obach, R. S.; Maurer, T. S. *Curr. Drug Metab.* **2007**, *8*, 407.
16. Tang, W.; Stearns, R. A.; Wang, R. W.; Miller, R. R.; Chen, Q.; Ngui, J.; Bakshi, R. K.; Nargund, R. P.; Dean, D. C.; Baillie, T. A. *Xenobiotica* **2008**, *38*, 1437.
17. Cerny, M. A.; Hanzlik, R. P. *Arch. Biochem. Biophys.* **2005**, *436*, 265.
18. (a) Nakahira H.; Nishio, Y.; Kimura, H.; World Patent 2009084497, 2009; (b) Nishio, Y.; Kimura, H.; Tosaki, S.; Sugaru, E.; Sakai, M.; Horiguchi, M.; Masui, Y.; Ono, M.; Nakagawa, T.; Nakahira, H. *Bioorg. Med. Chem. Lett.* **2010**, *20*, 7246.
19. Nelson, T. D.; Rosen, J. D.; Smitrovich, J. H.; Payack, J.; Craig, B.; Matty, L.; Huffman, M. A.; McNamara, J. *Org. Lett.* **2005**, *7*, 55.
20. Nishio, Y.; Uchiyama, K.; Kito, M.; Nakahira, H. *Tetrahedron* **2011**, *67*, 3124.
21. (a) Ma, B.; Prueksaritanont, T.; Lin, J. H. *Drug Metab. Dispos.* **1999**, *28*, 125; (b) Hollenberg, P. F.; Kent, U. M.; Bumpus, N. N. *Chem. Res. Toxicol.* **2008**, *21*, 189.
22. Obach, R. S.; Walsky, R. L.; Venkatakrishnan, K. *Drug Metab. Dispos.* **2006**, *35*, 246.
23. Kowalchick, J. E.; Leiting, B.; Pryor, K. D.; Marsilio, F.; Wu, J. K.; He, H.; Lyons, K. A.; Eiermann, G. J.; Petrov, A.; Scapin, G.; Patel, R. A.; Thornberry, N. A.; Weber, A. E.; Kim, D. *Bioorg. Med. Chem. Lett.* **2007**, *17*, 5934.
24. McDonald, J. K.; Leibach, F. H.; Grindeland, R. E.; Ellis, S. *J. Biol Chem.* **1968**, *243*, 4143.
25. Abbott, C. A.; Yu, D. M.; Woollatt, E.; Sutherland, G. R.; McCaughan, G. W.; Gorrell, M. D. *Biochem* **2000**, *267*, 6140.
26. Olse, C.; Wagtmann, N. *Gene* **2002**, *299*, 185.
27. (a) Lankas, G. R.; Leiting, B.; Sinha Roy, R.; Eiermann, G. J.; Beconi, M. G.; Biftu, T.; Chan, C.-C.; Edmondson, S.; Feeney, W. P.; He, H.; Ippolito, D. E.; Kim, D.; Lynos, K. A.; Ok, H. O.; Patel, R. A.; Petrov, A. N.; Pruor, K. A.; Qian, X.; Reigle, L.; Woods, A.; Wu, J. K.; Zaller, D.; Zhang, X.; Zhu, L.; Weber, A. E.; Thronberry, N. A. *Diabetes* **2005**, *54*, 2988; (b) Burkey, B. F.; Hoffmann, P. K.; Hassiepen, U.; Trappe, J.; Juedes, M.; Foley, J. E. *Diab. Obes. Metab.* **2008**, *10*, 1057; (c) Wu, J.-J.; Tang, H.-K.; Yeh, T.-K.; Chen, C.-M.; Shy, H.-C.; Chu, Y.-R.; Chien, C.-H.; Tsai, T.-Y.; Huang, Y.-C.; Huang, Y.-L.; Huang, C.-H.; Tseng, H.-Y.; Jiaang, W.-T.; Chao, Y.-S.; Chen, X. *Biochem. Pharmacol.* **2009**, *78*, 203.
28. Scanlan, M. J.; Raj, B. K. M.; Calvo, B.; Garin-Chesa, P.; Sanz-Moncasi, M. P.; Healey, J. H.; Old, L. J.; Rettig, W. J. *Proc. Natl. Acad. Sci. U.S.A.* **1994**, *91*, 5657.